

Wellbore associated problems due to gas injection into non-horizontal structures

A. Chamani*, V. Rasouli

Department of Petroleum Engineering, Curtin University, 6151Perth, Australia

Received 26 May 2012; received in revised form 20 November 2012; accepted 01 January 2013
*Corresponding author: amin.chamani@postgrad.curtin.edu.au (A. Chamani).

Abstract

The rapid growth in natural gas consumption has increased the need for gas storage, in particular in the form of injection into depleted reservoirs. Also, CO₂ sequestration into the depleted reservoirs has attracted a large attention recently. However, it is important to ensure that the injection pressure is maintained below a certain limit to avoid unsealing the cap rock or reactivation of any existing fracture planes within or above the reservoir rocks. In particular, it can be thought that gas injection into formations with non-horizontal structures, such as anticlines, is more problematic than horizontal formations due to the development of shear zones in such structures. This could potentially result in long term wellbore problems such as casing collapse or shearing along a fault or fracture plane intersecting the wellbore. In this study we compare the stress profile changes before and after gas injection into three structures: a horizontal and two anticlines with different slopes at their flanks. For this purpose a 3D numerical simulator was used. The program was developed using finite element method (FEM) and the code was written in Fortran. The stress magnitudes along curved profiles were compared for three structures at a similar depth. A limited extension of a porous zone was assumed in this study. The results indicate how as structure becomes more curvy in its geometry the likelihood of shear displacement increases. This is significantly important for well design purposes as it could reactivate any existing fault or fracture planes and result in cutting the wellbore or causing casing collapse.

Keywords: *Well design, CO₂ sequestration, gas injection, reservoir, Geomechanics, fracture reactivation.*

1. Introduction

During the last decades a growing dependency of countries on natural gas as a source of energy has taken place in both domestic consumers and infrastructure. Natural gas has some special features that enhance the need of available storage for it in parallel to its direct production or import [1]. There are three main types of natural gas storage: storage in depleted hydrocarbon reservoirs, storage in aquifers and storage in leached salt caverns. However, short term gas storage is also needed in coal seam gas (CSG) projects where the CSG is fed into the LNG plant, for example the Galilee basin in Queensland

Australia [2]. Also, limited cases are available where storage in caverns made of hard rocks are reported. Platt (2009) presented a comprehensive review on different types of natural gas storage and outlined their advantages and disadvantages [3].

The history of underground gas storage activities dates back to the storage site in a depleted gas reservoir in Welland County, Ontario (Canada) in 1915 [4]. Afterward until the 1950s almost all gas storage activities were undertaken in the depleted gas reservoirs and currently nearly 81.6 % of all worldwide activities are in depleted hydrocarbon

reservoirs [5]. The majority of the past storage cases are in depleted gas field instead of depleted oil field [5].

Production from a reservoir or injection of gas into a reservoir for storage purposes causes a change in effective stresses. This will result in volumetric changes of the formations and therefore formation compaction or uplift, respectively [6]. Figure 1.a shows schematically the stress magnitude changes due to compaction in a porous formation. As a result of compaction, as is shown in Figure 1.a for non-flat overburden layers the crestal section experiences an increase in horizontal stress; whereas a reduction in the remote flank is expected. The rocks above the shoulders will undergo a shear stress regime. More production of oil/gas from the porous formation means further stress redistribution in the overburden layers and therefore if the induced shear stress (mostly above the shoulders) exceeds

the shear strength of the existing fracture (or the bedding planes) sliding of fracture plane (or interbeds) may happen. Looking at Figure 1.a, it is likely that a fracture or fault plane oriented favorably in the flank section to get reactivated. This may result in sharing a wellbore which is cut by this fault or fracture plane. Similarly, a cased hole may experience dogleg shape or collapse (Figure 1.b) if the wellbore is drilled in this location of the anticline [6].

On the other hand, CO₂ sequestration had drawn remarkable attention during the two last decades according the greenhouse gas effects. Geological carbon dioxide sequestration is performed in depleted oil and gas reservoir, deep aquifer, saline formation, and coal beds. For storage purposes cap rock sealing and fault reactivation are major concerns. There are at least three industrial project (with above 1 MtCO₂/yr) worldwide according to Table 1. Again in few cases injected layers completely horizontal and in reality layers are curved.

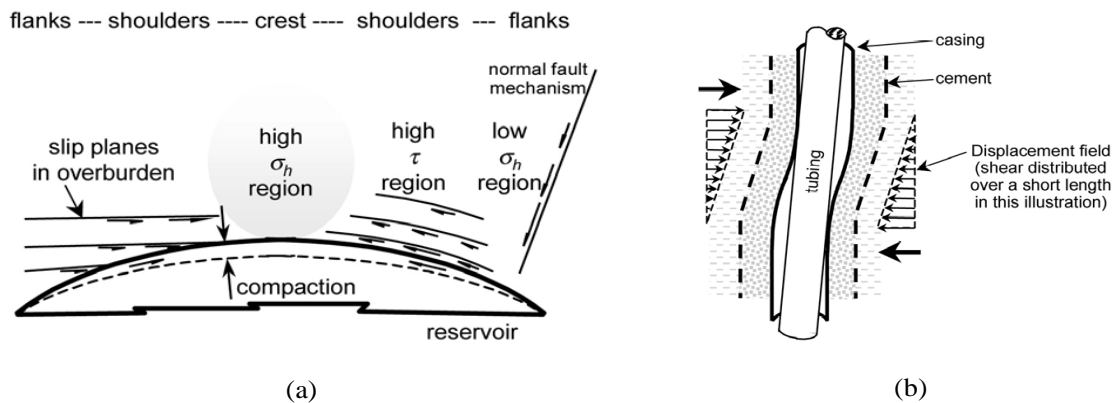


Figure 1. Shear stresses developed due to gas injection into an anticline structure (a); and (b) dogleg or collapse of casing [6].

Table 1. Industrial CO₂ storage site information [8]

Project name	Country	Injection start (year)	Approximate average daily injection rate (tCO ₂ day ⁻¹)	Total planned storage (tCO ₂)	Storage reservoir type
Weyburn	Canada	2000	3,000-5,0000	20e6	EOR *
In Salah	Algeria	2004	3,000-4,000	17e6	Gas Field
Sleipner	Norway	1996	3,0000	20e6	Saline Formation

* Enhanced oil recovery using CO₂

The above discussion demonstrates the importance of formation geometry with respect to the stress distribution before and after injection or depletion. In this study the effects of gas injection into formations with different geometries were investigated using a three-dimensional finite element program which was developed by the

authors at Petroleum Engineering Department of Curtin University. In the following sections after a brief introduction to the finite element simulation method the results of a 3D numerical simulation will be presented where the stress redistribution due to gas injection into three structures are compared.

2. Finite element simulation

Finite element method is very capable numerical tools to achieve an approximate solution for a specific structure under specific boundary conditions. In this numerical approach the structure domain is firstly discretised into finite number named "elements". Each element is characterized by its nodes defining its geometry and material properties. The displacement field is approximated inside each element as:

$$u \approx \hat{u} = \mathbf{N}u^e, \tag{1}$$

In this equation N is the shape functions matrix, and u^e is the nodal displacement vector of element. (Bold-face letters indicate vector or matrix).

Shape functions have two important characteristics:

$$N_i(x_i) = I \text{ at node } i \tag{2}$$

$$N_i(x_j) = 0; i \neq j \text{ at other nodes} \tag{3}$$

Based on displacement vector the strain tensor entities can be determined by differentiation of displacement as

$$\boldsymbol{\varepsilon} = \mathbf{d}u = \mathbf{d}N\mathbf{u}^e = \mathbf{B}u^e \tag{4}$$

where d is the differentiation operator matrix and B is a matrix which relates strain tensor components to nodal displacement vector and contains the differentiate of shape functions.

We can determine the stress tensor now having the strain tensor as

$$\boldsymbol{\sigma} = \mathbf{D}\boldsymbol{\varepsilon} \tag{5}$$

where D is the elasticity matrix.

According to principle of virtual work for any permissible small virtual deformation the virtual work done by external loads is equal to the virtual energy of internal stresses inside the element. Considering an element under the nodal action p and body force F , the virtual energy due to the internal stresses is:

$$\delta W_{\text{internal stress}} = \int_{V^e} \delta \boldsymbol{\varepsilon}^T \boldsymbol{\sigma} dv = \int_{V^e} \delta \mathbf{u}^{eT} \mathbf{B}^T \boldsymbol{\sigma} dv = \int_{V^e} \delta \mathbf{u}^{eT} \mathbf{B}^T \mathbf{D} \mathbf{B} \mathbf{u}^e dv \tag{6}$$

The virtual work due to external loads of nodal actions and body forces is

$$\delta W_{\text{external loads}} = \delta \mathbf{u}^{eT} \mathbf{p} + \int_{V^e} \delta \mathbf{u}^T \mathbf{F} dv = \delta \mathbf{u}^{eT} \mathbf{p} + \int_{V^e} \delta \mathbf{u}^{eT} \mathbf{N}^T \mathbf{F} dv \tag{7}$$

According to the principle of virtual work:

$$\int_{V^e} \delta \mathbf{u}^{eT} \mathbf{B}^T \mathbf{D} \mathbf{B} \mathbf{u}^e dv = \delta \mathbf{u}^{eT} \mathbf{p} + \int_{V^e} \delta \mathbf{u}^{eT} \mathbf{N}^T \mathbf{F} dv \tag{8}$$

which leads to:

$$\left(\int_{V^e} \mathbf{B}^T \mathbf{D} \mathbf{B} dv \right) \mathbf{u}^e = \mathbf{p} + \int_{V^e} \mathbf{N}^T \mathbf{F} dv, \tag{9}$$

The coefficient matrix $\left(\int_{V^e} \mathbf{B}^T \mathbf{D} \mathbf{B} dv \right)$ is called the element stiffness matrix \mathbf{K}^e and the integral of $\int_{V^e} \mathbf{N}^T \mathbf{F} dv$ is called equivalent nodal force due to body forces.

Afterward based on the calculated stiffness matrix, displacement vector and nodal force vector of all elements of entire the structure the corresponding global matrix and vectors are formed during a process named "assemblage". This process results in the formation of linear equations system which needs to be solved. In our developed three-dimensional finite element program the final system of linear equation is solved based on Gaussian elimination method.

The computational process and algorithm of finite element simulation method based on above formulations is shown in Figure 2.

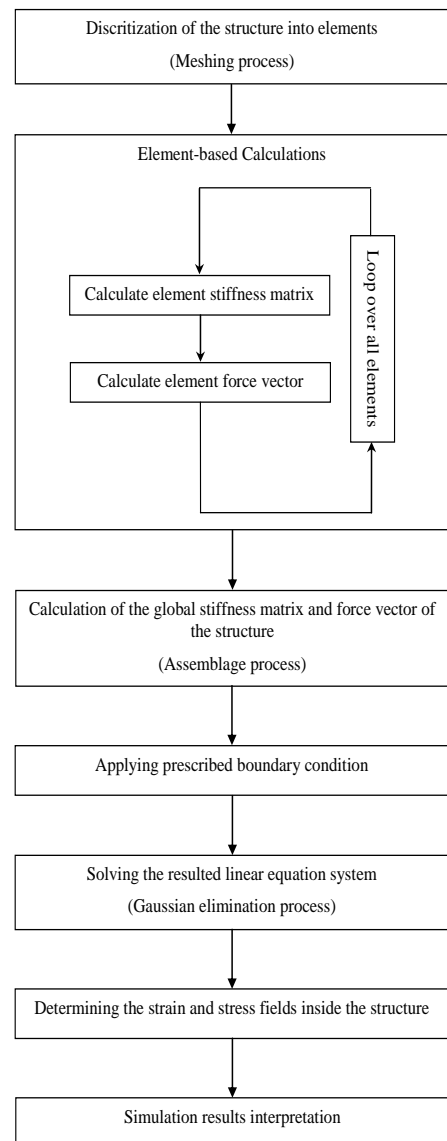


Figure 2. Flowchart of numerical simulation based on finite element method for structural analysis.

3. Model geometry and properties

A horizontal layered and two anticline models with different slopes at their flanks were used for the purpose of this study. The geometries of these models are shown in Figure 3. All geometries have similar thickness (of 40 m) and horizontal extensions. The depth of the highest point of the layer to the surface is 500 m, and the horizontal extension of the injected zone is 200 m (i.e. from $x=400\text{m}$ to $x=600\text{m}$). The material used for the analyses has a density of 2500 kg/m^3 , a Young's modulus of 10 GPa and a Poisson's ratio of 0.25 . The Biot's coefficient was assumed to be 1.0 . We used refining of elements closer to the injected zone in order to enhance the finite element modeling results as can be seen in Figure 3. The reservoir zone was injected up to 3.0 MPa and the induced stresses estimated. All the models characteristics including geomaterial properties, depth of the porous zone and maximum injection pressures correspond to a real injection site. The strike of these structures assumed to be parallel to y -axis. The three-dimensional models are restricted in their deformations normal to the plane in all lateral planes and bottom side while vertical sliding of the lateral planes are permitted. The effect of gravitational loading was discarded from the results to only record the injection-induced effects. In Figure 3, profiles are shown along which the stress redistribution after gas injection was compared. As is seen from this figure these profiles are curved geometry in case of anticline structures. In the subsequent sections the simulation results are presented and discussed.

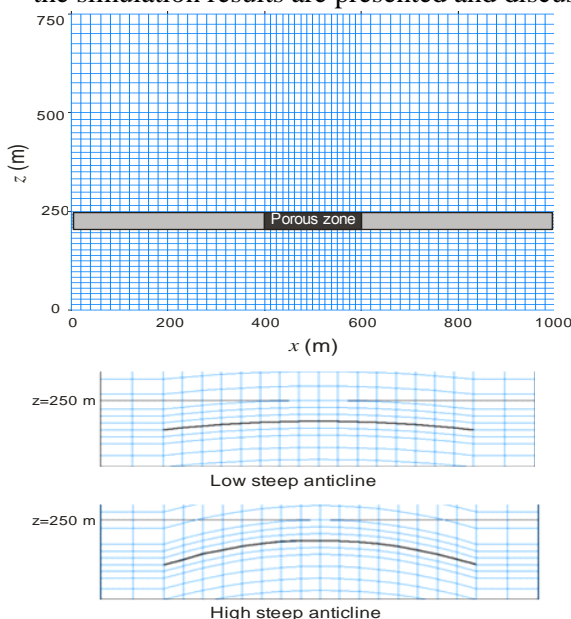


Figure 3. A 2D section of mesh generated for horizontal structures S1 (top) and anticlines S2 (middle) and S3. The stress redistribution was modeled along the shown profiles.

4. Results and discussion

4.1. Contours of injection- induced stresses

The simulations were performed to determine the induced stresses due to gas injection into the reservoir formations. As an example, Figure 4 shows vertical (σ_{zz}), horizontal (σ_{xx}) and shear (σ_{zx}) induced stresses corresponding to structure S3, i.e. the high steep anticline. Further details of the stress contours for other two structures can be found in [7].

The injection-induced shear stress (σ_{zx}) is the most likely component which will be affected by the geometry of the structure. From practical point of view the magnitude of this stress is used to evaluate the potential for fault or fracture reactivation and sliding of the interbeds with low cohesion along each other: this may result in loss of uncased wellbore in short term period after drilling or collapse of casing in long term production from the reservoir. From Figures 4 it is seen that the magnitude of the shear stress component (σ_{zx}) increases at the corners when the structure deviates from being horizontal ($7.86 \times 10^5\text{ pa}$). This result is expected due to stress concentration at sharp corners. However, the more important conclusion is the development of the shear stress zone at the flank area of the anticline structures. The latter result may be attributed to the curvature of the structure but not to stress concentration due to sharp corners. This conclusion suggests avoiding drilling wellbores at the flank areas in curved structures such as anticlines as the possibility of interbeds movement and reactivation of any existing fracture plane is high due to large shear stresses applied in these zones.

4.2. Contours of injection- induced stresses

In Figure 5 two profiles along which the injection induced shear stresses were extracted are shown. The horizontal profile passing through the center of the injected zone at $z=230\text{ m}$ whereas the vertical profile passing through the center of the flank at $x=450\text{ m}$. The reason for choosing the vertical profile at this location instead of the center of the structure (i.e. at $x=500\text{ m}$) is that the shear stress would be negligible along the profile passing through the center of the porous zone whereas remarkable shear stresses induced along profiles off from the center line which is due to the curved geometry of the model. The corresponding results for three structures S1, S2 and S3 are plotted in Figures 6 and 7, respectively.

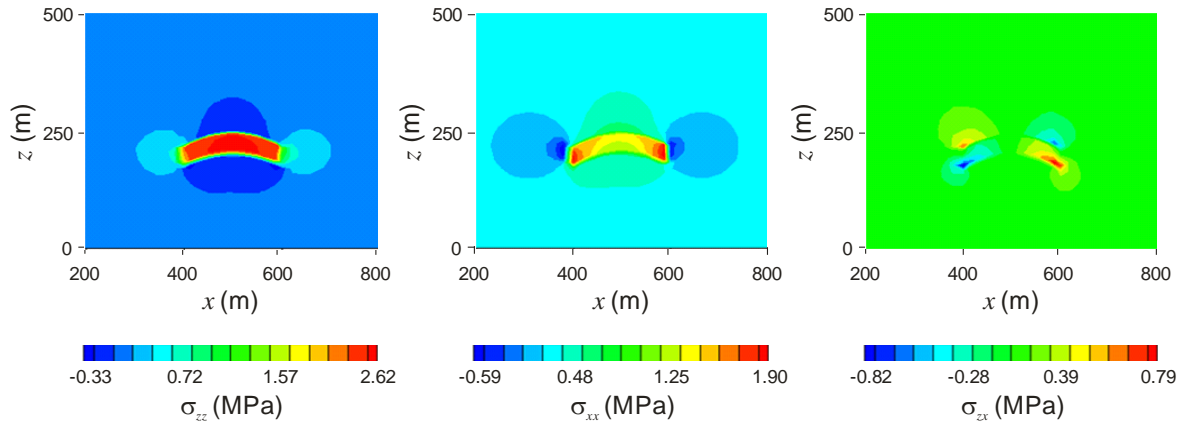


Figure 4. Injection-induced vertical (left), horizontal (middle) and shear stress contours for anticline structure S3.

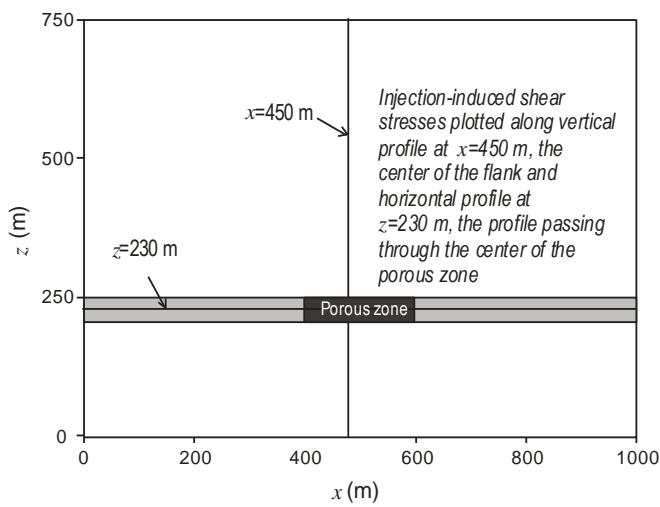


Figure 5. Injection-induced shear stresses were determined along a vertical and horizontal profile passing through the center of the porous zone for three structural models of S1 to S3.

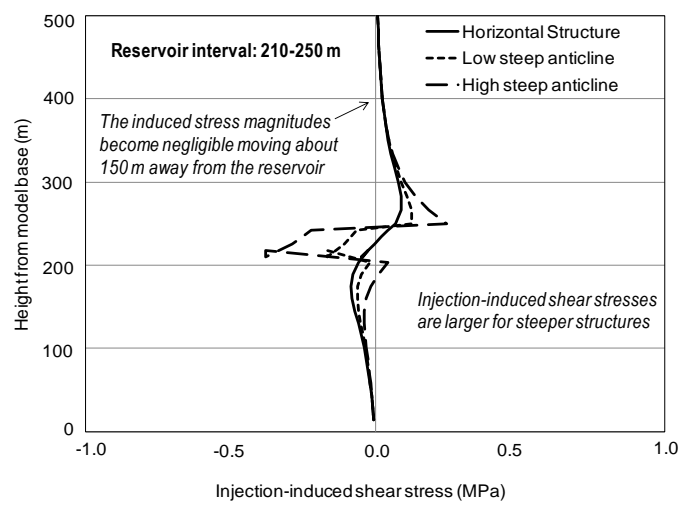


Figure 6. Injection-induced stresses along profile at $x=450$ m corresponding to three structural models of S1, S2 and S3.

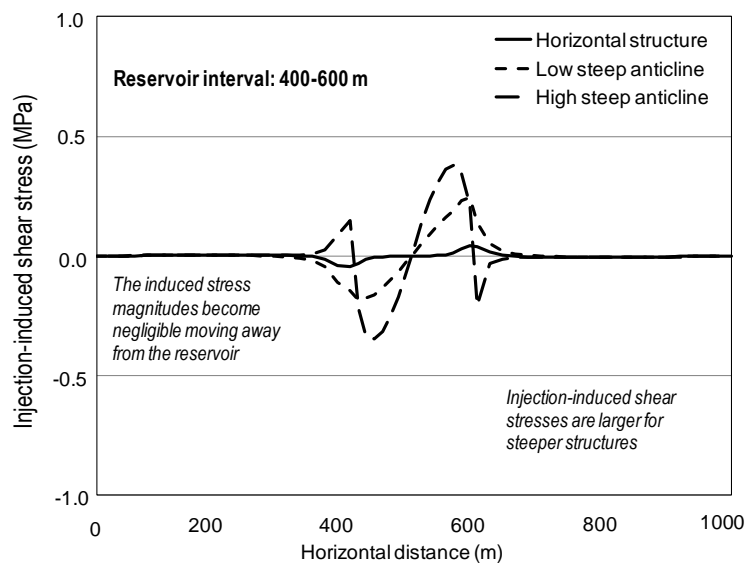


Figure 7. Injection-induced stresses along profile at $z=230$ m corresponding to three structural models of S1, S2 and S3.

The results of Figure 6 indicate that shear stresses become nearly negligible at distances larger than approximately 150 m away from the center of the reservoir in vertical direction, i.e. towards over/under burden. This result is valid for the parameters used in this study and may change if model properties are changed. The results of Figure 7 indicate that the shear stresses are larger at both sides of the reservoir, i.e. $x=400$ m and 600 m. The results of both figures demonstrate that the steeper the formation structure the larger the magnitude of induced shear stresses and the larger its extension zone will be.

Finally, the injection induced shear stresses were estimated along two curve profiles as shown in Figure 3 and compared against the stresses along the horizontal profile at the center of the porous zone. The results of this analysis are shown in Figures 8. From this figure, again, it is seen that for the horizontal structure the shear stress only appears at corners of the porous zone, yet it is very minor and negligible. For anticline structures shear stresses not only appears at the corners but also exist within the porous zone too and its magnitude is a direct function of the slope of the anticline. The results indicate clearly the potential impact of the induced shear stresses on a wellbore drilled at the flank of the anticline and the subsequent problems including fault or fracture reactivation or casing collapse during the life of the reservoir.

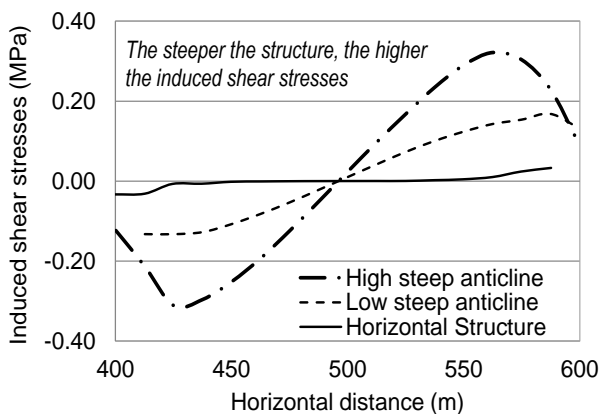


Figure 8. Injection-induced shear stresses: horizontal profile for S1 and curved profiles for structural models of S2 and S3.

It is important to note the difference between the injection-induced shear stresses estimated along horizontal (Figure 7) and curved (Figure 8) profiles. Due to the curved structure geometry of the anticlines linear profiles not necessarily represent similar formations but it can pass through different layers. This means that the stress changes in this case could be due to change in formation properties as well as geometry effects.

However, by choosing curved profiles passing within the layer it is ensured that we only consider the changes in stress distribution due to the geometry effect. However, in this study, both results indicate remarkable changes in shear stress distribution due to gas injection.

5. Conclusions

In this paper the changes in stress distribution due to gas injection into a horizontal and two anticline structures with different slopes were studied. The stress magnitudes along both horizontal and curved profile geometries were analyzed. The results indicated that the injection induced shear stresses for horizontal layers are at the corner of the porous zone and their magnitude is insignificant. However, the magnitude of shear stresses becomes significant, in particular at the corners of the porous zone, as the slope of the anticline structure increases. This means that a fault or fracture plane existing at the flank of the formation would be prone to reactivation and this could potentially result in loss of a wellbore had it been drilled in this zone. Similarly, for cased wellbores, this shearing induced stress may result in casing collapse. The results demonstrate the importance of having a good knowledge of stress redistribution with respect to the formation structure throughout the entire life of a reservoir.

References

- [1]. Havard, J., and R. French. (2009). The importance of gas storage to the UK: The DECC perspective. Geological Society, London, Special Publications, 313, 13-15.
- [2]. Holland, J. R., J. K. Applegate. (2008). Recent Coalbed Methane Exploration in the Galilee Basin, Queensland, Australia. International Coalbed & shale Gas Symposium.
- [3]. Plaats, H. (2009). Underground gas storage — why and how. Geological Society, London, Special Publications, 313, 25-37.
- [4]. Evans, D. J. (2009). A review of underground fuel storage events and putting risk into perspective with other areas of the energy supply chain. Geological Society, London, Special Publications, 313, 173-216.
- [5]. Davidson, M. (2009). Underground gas storage project at Welton oilfield, Lincolnshire: Local perspectives and responses to planning, environmental and community safety issues. Geological Society, London, Special Publications, 313, 149-162.
- [6]. Dusseault M.B., M.S. Bruno and J. Barrera (2001). Casing shear: causes, cases, cures. The SPE Int Oil and Gas Conference.

[7]. Rasouli, V., and Chamani, A., (2011). A 3D numerical study on Geomechanical response of a structural reservoir due to gas injection.GP086, GeoProc2011 conference, Perth, Western Australia, July 6-9, (2011).

[8]. Edward Rubin, Leo Meyer, Heleen de Conick,(2005). Carbon Dioxide Capture and Storage, Technical Summary. www.ipcc.ch/pdf/special-reports/srccs/srccs_technicalsummary.pdf